Bioconjugate Chemistry

Article

pubs.acs.org/bc

Novel Isoprenoyl Nanoassembled Prodrug for Paclitaxel Delivery

Simona Mura,*[,†,‡] Fatima Zouhiri,[†,‡] Stephanie Lerondel,[§] Andrei Maksimenko,[†,‡] Julie Mougin,[†,‡] Claire Gueutin,[†,‡] Davide Brambilla,[†,‡] Joachim Caron,[†,‡] Eric Sliwinski,[†,‡] Alain LePape,[§,∥] Didier Desmaele,[†,‡] and Patrick Couvreur*[,†,‡]

[†]Université Paris-Sud, Faculté de Pharmacie, 5 rue Jean-Baptiste Clément, 92296 Châtenay-Malabry cedex, France

[‡]CNRS UMR 8612, Institut Galien Paris-Sud, 5 rue Jean-Baptiste Clément, 92296 Châtenay-Malabry cedex, France

[§]TAAM-UPS44, CIPA, CNRS Orléans, F-45071 Orléans, France

[∥]Research Center for Respiratory Diseases, Inserm U11OO/EA 6305, Université François Rabelais, F-37032 Tours, France

Supporting Information

ABSTRACT: A new paclitaxel (Ptx) prodrug was designed by coupling a single terpene unit (MIP) to the hydroxyl group in position 2′ of the drug molecule. Using a squalene derivative of polyethylene glycol (SQ-PEG) as surface active agent, the resulting bioconjugate (PtxMIP) self-assembled in water leading to the formation of stable nanoparticles (PtxMIP_SQ-PEG NPs) with an impressively high drug loading (82%). *In vivo*, the anticancer activity of this novel Ptx nanoassembled prodrug was compared to the conventional Cremophor-containing formulation (Taxol) on a murine model of breast cancer lung metastasis induced by intravenous injection of 4T1 tumor cells, genetically modified to stably express firefly luciferase. Cell growth was assessed noninvasively by bioluminescence imaging (BLI) which enabled monitoring tumor metastatic burden in the same animals. PtxMIP_SQ-PEG nanoparticles slowed metastatic spread and were better tolerated than the Cremophor-containing formulation (i.e., free drug), thus demonstrating the potential of terpene-based nanoassembled prodrugs in the improvement of the therapeutic index of Ptx in balb/c mice.

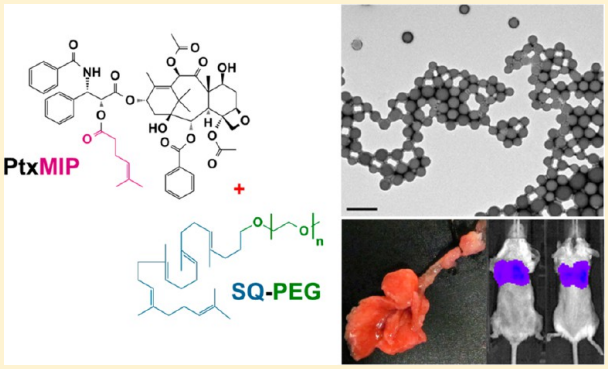

INTRODUCTION

Paclitaxel (Ptx) is a naturally occurring diterpene alkaloid originally isolated in the 1960s from the bark of the Pacific Yew tree (*Taxus brevifolia*).[1] Ptx is a unique antimitotic agent able to promote assembly of tubulin into extraordinary stable microtubules, which are resistant to depolymerization. On the basis of this action, it causes arrest of the cell cycle in the late G2/M phase,[2,3] which is the main mechanism of its toxicity. Although the therapeutic potential of Ptx as anticancer agent is important (action in the nanomolar range), its widespread use is compromised by limited water solubility (<3 $\mu g.mL^{-1}$)[4] and the absence of functional groups which would enable salt formation. The currently clinically used formulation (Taxol) consists of a Ptx emulsion in a mixture of Cremophor EL (polyoxyl 35 castor oil) and absolute ethanol (50/50 v/v), then diluted, prior to intravenous administration, with saline or 5% dextrose solution[5] which, however, shows short-term physical stability and tends to precipitate. In addition, several studies demonstrated that the use of this nonionic solubilizer and emulsifier is associated with the insurgency of several side effects such as hypersensitivity reactions, hematological toxicity, peripheral neurotoxicity and neuropathy.[5−7] Despite the premedication with corticosteroids and antihistamines,[8,9] adverse reactions are often observed in 1−3% of patients.[10] Furthermore, it has been reported that the formation of Cremophor micelles, which sequestrate the Ptx, reduces the free fraction of the drug and may hamper tissue penetration.[11−13]

Several attempts have been made with the aim to develop a suitable alternative to the oil/ethanol vehicle enabling intravenous administration of therapeutic doses of Ptx, while overcoming the toxicity issues related to the use of Cremophor. Thus, Ptx has been formulated in a large variety of nanoscaled colloidal carriers including emulsions,[14] liposomes,[15,16] micelles,[17−20] nanoparticles (NPs),[21−25] and dendrimers.[26,27]

Some of these new formulations are marketed or in clinical trials. For instance, albumin-bound Ptx nanoparticles (Abraxane) demonstrated better pharmacokinetics profiles and higher therapeutic efficacy compared to Taxol, and was approved by FDA in 2005 for the treatment of metastatic breast cancer after failure of combination chemotherapy.[28,29] Another formulation, Genexol-PM, which consists of Ptx-loaded polymeric micelles,

Received: April 23, 2013
Revised: September 17, 2013
Published: September 30, 2013

   dx.doi.org/10.1021/bc400210x | *Bioconjugate Chem.* 2013, 24, 1840−1849

is currently in phase II clinical study and has already exhibited promising results.[30] Nevertheless, due to the low drug loading and the problems associated with the potential initially high rate of drug release from these colloidal formulations (that is, the burst release), the prodrug approach has been proposed as a valuable strategy to design water-soluble derivatives and to achieve improvements over the conventional formulation. Several prodrugs have been synthetized by covalent conjugation of various molecules to the hydroxyl group in position C7 or C2′ of Ptx. Position C2′ is widely used for derivatization due to the critical role of this hydroxyl group for the microtubule assembly activity. Prodrugs in which this position is engaged in covalent modifications are thus inactive, due to loss of the tubulin polymerization activity, and require *in vivo* hydrolysis to release the active molecule.[31−36] Water-soluble Ptx prodrugs have been created by coupling small molecules such as amino acids,[37] carboxylic acid,[31,38] sulfonate,[39] phosphate,[40,41] or sugar derivatives.[42,43] In order to achieve a controlled drug delivery to the site of action, macromolecular prodrugs in which the Ptx is linked to polysaccharides,[44,45] peptides,[46−51] polymers,[52−54] and lipids[55−61] have also been developed. Ptx derivatives selectively targeted to the tumor tissues were designed as well.[62] Among the fatty acid derivatives, the docosahexaenoic-acid-Ptx prodrug (DHA-Ptx, Taxoprexin) reached phase III clinical trials for the treatment of metastatic malignant melanoma.[63] However, although it enabled increase of the maximum tolerated dose compared to Taxol, this DHA-Ptx formulation still contains 10% of Cremophor which, therefore, might give rise to some toxicity issues.[64,65]

In this context, in order to design a novel Cremophor-free Ptx formulation, we have previously conjugated Ptx to squalene (SQ), a natural triterpene, which has allowed to obtain nanoassemblies[66−68] but with a dramatically lower anticancer activity compared to the free drug.[69] An improved cytotoxic activity and an increased therapeutic index were, nevertheless, achieved after the introduction of a dienic spacer between the Ptx and the SQ molecule.[70] In the recent past, using gemcitabine as model drug, other isoprenoid-based prodrug nanoparticles have been designed by using for conjugation terpene molecules with a lower number of isoprene units compared to squalene,[71] or by growing polyisoprene chains from the anticancer drug molecule.[72] The remarkable results obtained *in vivo* on pancreatic adenocarcinoma bearing mice have clearly demonstrated the versatility of the "terpenoylation" approach.

In the current study, we designed a novel isoprenoyl nanoassembled prodrug for Ptx delivery. Bioconjugates were prepared by coupling Ptx to a single isoprene unit and their conanoprecipitation with polyethylene glycol conjugated to squalene (SQ-PEG) allowed the construction of nanoparticles with impressively high drug loading.

The anticancer activity of these paclitaxel-monoisoprenoyl (PtxMIP_SQ-PEG) nanoparticles was tested *in vitro* on various cancer cell lines and *in vivo* on a mouse model of breast cancer lung metastasis, obtained by intravenous injection of luciferase-expressing 4T1 cells in balb/c mice. Tumor progression was sensitively monitored in real time by noninvasive bioluminescence imaging (BLI).

EXPERIMENTAL SECTION

Paclitaxel was purchased from Sequoia Research Product Ltd. (UK). 2-Methyl-3-buten-2-ol, dicyclohexylcarbodiimide (DCC), trimethyl orthoacetate, and 3-[4,5-dimethylthiazol-2-yl]-3,5-diphenyl tetrazolium bromide (MTT) were purchased from Sigma-Aldrich Chemical Co., France. Chemicals obtained from commercial suppliers were used without further purification. Purity of tested compound was determined by elemental analysis to be >95% pure. IR spectra were obtained as solid or neat liquid on a Fourier Transform Bruker Vector 22 spectrometer. Only significant absorptions are listed. Optical rotations were measured on a Perkin-Elmer 241 Polarimeter at 589 nm. The ^{1}H and ^{13}C NMR spectra were recorded on Bruker Avance 300 (300 and 75 MHz, for ^{1}H and ^{13}C, respectively) or Bruker Avance 400 (400 and 100 MHz, for ^{1}H and ^{13}C, respectively) spectrometers. Recognition of methyl, methylene, methine, and quaternary carbon nuclei in ^{13}C NMR spectra rests on the *J*-modulated spin−echo sequence. Mass spectra were recorded on a Bruker Esquire-LC spectrometer. High-resolution mass spectra (ESI) were recorded on a ESI/TOF (LCT, Waters) LC-spectrometer. Elemental analyses were performed by the Service de microanalyse, Centre d'Etudes Pharmaceutiques, Châtenay-Malabry, France, with a Perkin-Elmer 2400 analyzer. The sizes of the obtained nanoassemblies were measured using a Malvern particle size analyzer (Zetasizer). Analytical thin-layer chromatography was performed on Merck silica gel $60F_{254}$ glass precoated plates (0.25 mm layer). Column chromatography was performed on Merck silica gel 60 (230−400 mesh ASTM). CH_2Cl_2 was distilled from calcium hydride, under a nitrogen atmosphere. All reactions involving air- or water-sensitive compounds were routinely conducted in glassware which was flame-dried under a positive pressure of nitrogen.

Synthesis of 5-Methyl-hex-4-enoic Acid (3). A mixture of 2-methyl-3-buten-2-ol (20.5 g, 0.23 mol) and 1 mL of propionic acid in trimethyl orthoacetate (200 mL) was heated at 140 °C during 4 h. The reaction mixture was slowly added into an ice-cooled 1 N HCl solution (300 mL) and the mixture was extracted with ethyl acetate (3 × 100 mL). The combined organic layers were washed with aqueous sodium bicarbonate, then brine, dried over $MgSO_4$, and concentrated under reduced pressure to leave an oil which was distilled under reduced pressure (bp 75−80 °C, 15 mmHg) to afford 5-methyl-hex-4-enoic acid methyl ester (24.2 g, 65%) as a colorless oil. A solution of the above ester (20.0 g, 0.14 mol) in methanol (150 mL) was treated with 3 N NaOH (50 mL) and the resulting mixture was stirred at reflux for 1 h. The mixture was concentrated under reduced pressure and the residue was acidified with 6 N HCl to pH 2. The resulting mixture was extracted with ether. The organic layer was dried over $MgSO_4$, and the solvent was removed to leave a yellow oil **3** which was distilled under reduced pressure (bp 120−125 °C, 15 mmHg) to provide the acid **3** (15.2 g, 85%) as a colorless oil.[73] ^{1}H NMR (300 MHz, $CDCl_3$) δ 10.5−8.5 (broad, 1H, OH), 5.15−5.08 (m, 1H, $(CH_3)_2C{=}CH$), 2.50−2.25 (m, 4H, $CH_2CH_2CO_2H$), 1.70 (s, 3H, $(CH_3)_2C{=}CH$), 1.63 (s, 3H, $(CH_3)_2C{=}CH$); ^{13}C NMR (75 MHz, $CDCl_3$) δ: 179.8 (C, CO_2H), 133.4 (C, $(CH_3)_2C{=}CH$), 122.1 (CH, $(CH_3)_2C{=}CH$), 34.2 (CH_2, CH_2CO_2H), 25.6 (CH_3, $(CH_3)_2C{=}CH$), 23.3 (CH_2, $CH_2CH_2CO_2H$), 17.6 (CH_3, $CH_3)_2C{=}CH$).

Synthesis of Paclitaxel Conjugate (2, PtxMIP). To a solution of Paclitaxel (**1**) (761 mg, 0.89 mmol) in dry CH_2Cl_2 (10 mL) were sequentially added at 0 °C acid **3** (120 mg, 0.93 mmol), DMAP (109 mg, 0.89 mmol), and DCC (550 mg, 2.67 mmol). The reaction mixture was stirred at 0 °C for 3 h and then 2 h at room temperature. The mixture was filtered, and the solid washed with CH_2Cl_2. The filtrate was concentrated under

Scheme 1. Synthesis of Prodrug 2

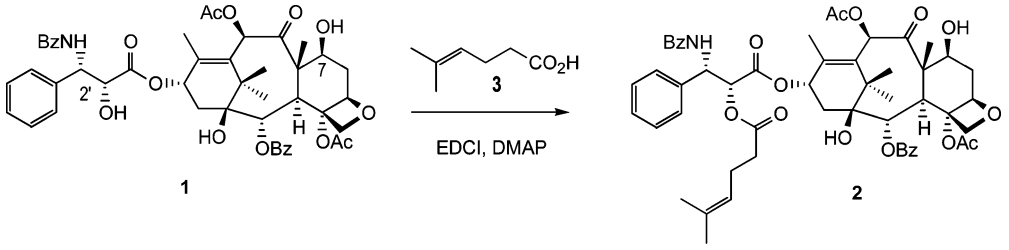

reduced pressure and the residue was purified by column chromatography on silica gel eluting with AcOEt/petroleum ether, 1:2, to give a white solid. Recrystallization in diethyl ether at −20 °C yielded conjugate **2** a white fluffy solid (537 mg, 62%). (Scheme 1). Mp: 146−150 °C (Et_2O). $[\alpha]_D^{21}$ = −1.7 (c = 1.5, $CHCl_3$); IR (neat): ν = 3500−3100, 3000−2900, 1744, 1724, 1714, 1638, 1538, 1451, 1375, 1270, 1240, 1177, 1143, 1110, 1070, 1049, 1026, 982, 904, 710, 701; ^{1}H NMR (400 MHz, $CDCl_3$). Applying conventional taxoid numbering δ: 8.14 (d, J = 7.1 Hz, 2H, $PhCO_2$), 7.73 (d, J = 7.1 Hz, 2H, PhCONH), 7.61 (t, J = 7.1 Hz, 1H, $PhCO_2$), 7.55−7.46 (m, 3H, C*H*-ar), 7.45−7.31 (m, 7H, C*H*-ar), 6.89 (d, J = 9.3 Hz, 1H, N*H*), 6.30 (s, 1H, H-10), 6.26 (t, J = 8.4 Hz, 1H, H-13), 5.96 (dd, J = 9.3 Hz, J = 3.2 Hz, 1H, H-3′), 5.68 (d, J = 6.9 Hz, 1H, H-2), 5.52 (d, J = 3.2 Hz, 1H, H-2′), 5.01 (td, J = 7.0 Hz, J = 1.3 Hz, 1H, $(CH_3)_2C{=}CH$), 4.98 (dd, J = 9.9 Hz, J = 1.7 Hz, 1H, H-5), 4.45 (dd, J = 9.0 Hz, J = 7.9 Hz, 1H, H-7), 4.32 (d, J = 8.4 Hz, 1H, H-20), 4.20 (d, J = 8.4 Hz, 1H, H-20), 3.82 (d, J = 6.9 Hz, 1H, H-3), 2.59 (1 H, s, O*H*), 2.60−2.10 (m, 6H, 1H-14, 1H-6, $=CHCH_2CH_2CO_2$Ptx), 2.45 (s, 3H, CH_3CO_2), 2.24 (s, 3H, CH_3CO_2), 1.94 (s, 3H, H-18), 1.95−1.83 (m, 1H, H-6), 1.68 (s, 3H, H-19), 1.66 (s, 3H, $CH{=}C(CH_3)_2$), 1.59 (s, 3H, $CH{=}C(CH_3)_2$), 1.26 (s, 3H, H-16), 1.13 (s, 3H, H-17); ^{13}C NMR (100 MHz, $CDCl_3$) δ: 203.9 (C, C-9), 172.3 (C, $PtxO_2CCH_2CH_2CH{=}$), 171.2 (C, CH_3CO_2), 169.8 (C, CH_3CO_2), 168.1 (C, C-1′), 167.1 (2C, PhCONH, $PhCO_2$), 142.8 (C, C-12), 137.0 (C, C-ar), 133.8 (C, C-ar), 133.7 (CH, CH-ar), 133.6 (C, $(CH_3)_2C{=}CH$), 132.8 (C, C-11), 132.0 (CH, CH-ar), 130.2 (2CH, CH-ar), 129.2 (C, C-ar), 129.0 (2CH, 2CH-ar), 128.7 (4CH, CH-ar), 128.4 (CH, CH-ar), 127.1 (2CH, CH-ar), 126.5 (2CH, CH-ar), 121.7 (CH, $(CH_3)_2C{=}CH$), 84.5 (CH, C-5), 81.1 (C, C-4), 79.2 (C, C-1), 76.5 (CH_2, C-20), 75.6 (CH, C-10), 75.1 (CH, C-2), 73.8 (CH, C-2′), 72.1 (CH, C-7), 71.7 (CH, C-13), 58.5 (C, C-8), 52.8 (CH, C-3′), 45.6 (CH, C-3), 43.2 (C, C-15), 35.6 (CH_2, C-6 or C-14), 35.5 (CH_2, C-6 or C-14), 33.9 (CH_2, $CH_2CH_2CO_2$Ptx), 26.8 (CH_3, C-16), 25.6 (CH_3, $(CH_3)_2C{=}CH$), 23.3 (CH_2, $CH_2CH_2CO_2$Ptx), 22.7 (CH_3, CH_3CO_2), 22.5 (CH_3), 22.1 (CH_3, C-17), 20.8 (CH_3, CH_3CO_2), 17.7 (CH_3, $(CH_3)_2C{=}CH$), 14.8 (CH_3, C-18), 9.6 (CH_3, C-19); HRMS (+ESI) m/z calc for $C_{54}H_{61}NO_{15}Na$ $[M+Na]^+$ 986.3933, found 986.3959; Anal. Calcd for $C_{54}H_{61}NO_{15}.2H_2O$, C 64.85, H 6.55, N 1.40; found, C 65.05, H 6.40, N 1.42. The synthesis of squalene coupled to polyethylene glycol (SQ-PEG, Trisnorsqualene-MePEG) has been achieved in 60% yield, as previously reported,[74] by alkylation of the sodium alkoxide of MePEG (MW 2000) with 1,1′,2-trisnorsqualenyl methanesulfonate.

Preparation of and Characterization of the Monoisoprenoyl Paclitaxel Nanoparticles (PtxMIP_SQ-PEG NPs). Four mg of compound **2** (PtxMIP) mixed with 320 μg of SQ-PEG (8%, w/w) were dissolved in ethanol (500 μL). The resulting solution was added dropwise under stirring (1000 rpm) into 1 mL of Milli-Q water. Formation of NPs occurred immediately. Ethanol was then evaporated at 30 °C *in vacuo* using a Rotavapor (Buchi Sarl, France) and the organic solvent-free colloidal dispersions of monoisoprenoyl Ptx nanoparticles (final concentration 4 mg.mL^{-1}) were stored at 4 °C. The NP diameter (Dz) was measured by dynamic light scattering (DLS) with a Nano ZS from Malvern (173° scattering angle) at 25 °C. The NP surface charge was investigated by ζ-potential measurement at 25 °C after dilution with 1 mM NaCl solution applying the Smoluchowski equation and using the same apparatus. Measurements were carried out in triplicate.

The surface (S) available for each PEG chain at the nanoparticle surface (also called ρPEG) is described by $S = (6Mn_{PEG})/(dN_A f\rho)$, with d the nanoparticle mean diameter, N_A the Avogadro number (6.022×10^{23} mol^{-1}), Mn_{PEG} the number-average molar mass of PEG, f the PEG weight fraction in the PtxMIP/SQ-PEG blend, and ρ the density of the nanoparticles (1.3 g.cm^{-3}). PEG distance represents the spatial gap between each PEG chain at the surface, calculated as $\sqrt{S}$.

The morphology of the monoisoprenoyl Ptx nanoparticles was examined by transmission electron microscopy (TEM) and cryogenic transmission electron microscopy (Cryo-TEM). For TEM imaging, 5 μL of NP dispersion at 4 mg.mL^{-1} was deposed on Formvar-Carbon coated grids (400 mesh). After 5 min at room temperature, the excess of volume was eliminated and the grids were observed with a JEOL 1400 120 kV electron microscope operating at 80 kV at a nominal magnification of 5000 to 40000. For negative staining, nanoparticles were stained with a 1% phosphotungstic acid solution filtered on 0.22 μm. Digital images were directly recorded on a CCD postcolumn high resolution (11 MegaPixel) high speed camera (SC1000 Orius, Gatan Inc.) using Digital Micrograph image acquisition and processing software (Gatan Inc.).

For Cryo-TEM observation, 5 μL of NP dispersion at 4 mg.mL^{-1} was deposited on a Lacey Formvar/carbon 300 mesh copper microscopy grid (Ted Pella). Most of the drop was removed with a blotting filter paper and the residual thin films remaining within the holes were vitrified after immersion in liquid ethane. The specimen was then transferred using liquid nitrogen to a cryo-specimen holder and observed using a JEOL FEG-2010 electron microscope.

Drug loading (expressed in %) was determined by using the following relationship: (weight Ptx) × 100/ (weight PtxMIP + weight SQ-PEG).

Colloidal and Chemical Stability of Monoisoprenoyl Paclitaxel Nanoparticles. The colloidal stability of PtxMIP_SQ-PEG NPs was investigated by measuring the nanoparticle mean diameter over a period of 21 days. PtxMIP_SQ-PEG NPs were diluted at a concentration of 0.4 mg.mL^{-1} with (i) water; (ii) cell culture medium (Dulbecco Modified Eagle's Medium (DMEM, Lonza, France)) supplemented with 10% of fetal bovine serum (FBS); (iii) sodium

acetate buffer 0.1 M (pH 4.5); (iv) sodium phosphate buffer 0.1 M (pH 7.4); or (v) sodium borate buffer 0.1 M (pH 9.1); and incubated at room temperature and at 37 °C.

The chemical stability of the paclitaxel−monoisoprenoyl conjugate was investigated in the presence of serum. Practically, PtxMIP_SQ-PEG NPs were incubated in human serum (Sigma Aldrich, France) (final concentration 0.4 mg.mL^{-1}) at 37 °C with gentle shaking. At various time points, aliquots (80 μL) were withdrawn and 5 μg of the internal standard (that is, freshly prepared *N*-octylbenzamide) was added to each sample. After addition of 820 μL of acetonitrile, aliquots were centrifuged (500*g*, 10 min, 4 °C). 20 μL of water was then added to 200 μL of supernatant and the released drug was quantified by HPLC analysis (Waters, Milford, MA 01757, USA). In order to avoid hydrolysis during sample workup, all sampled were stored at −20 °C until analysis. Briefly, the chromatographic system consisted of a Waters 1525 Binary LC pump, a Waters 2707 Autosampler, a Symmetry C18 column (5 μm, 39 × 150 mm, Waters), HPLC column temperature controllers (model 7950 column heater and chiller; Jones Chromatography, Lakewood, CO), and a Waters 2998 programmable photodiode-array detector. The HPLC column was maintained at 35 °C. Detection was monitored at 227 nm. The HPLC mobile phase was acetonitrile/water (55/45 v/v). Elution was carried out at a flow rate of 1 mL.min^{-1} isocratically for 7 min followed by a 20 min linear gradient to 95% acetonitrile. This was followed by a 8 min hold at 95% acetonitrile and a 2 min linear gradient back to acetonitrile/water (55/45 v/v). The system was held at acetonitrile/water (55/45 v/v) for 10 min for equilibration back to initial conditions.

Cell Culture. Human pancreatic carcinoma cell line MiaPaCa-2, lung carcinoma cell line A549, and breast adenocarcinoma cell line MCF7 were obtained from the American Type Culture Collection and maintained as recommended. Briefly, A549 cells were maintained in Roswell Park Memorial Institute medium (RPMI 1640 Lonza, France) supplemented with 10% FBS (Lonza, France). MiaPaCa-2 cells were grown in DMEM supplemented with 10% heat-inactivated (56 °C, 30 min) FBS and 2.5% heat-inactivated horse serum (Gibco, France). MCF7 cells were cultured in a mixture of DMEM/Ham's F12 (1:1) supplemented with 10% heat-inactivated FBS.

Luciferase-expressing murine breast adenocarcinoma cell line (4T1-luc2) was obtained from PerkinElmer (Roissy, France) and maintained in RPMI Glutamax medium (Gibco, France), supplemented with 20% D-glucose, 10 mM HEPES buffer, 1 mM sodium pyruvate, and 0.15% sodium bicarbonate (Gibco, France). All media were further supplemented with 50 U.mL^{-1} penicillin and 50 U.mL^{-1} streptomycin (Lonza, France). Cells were maintained in a humid atmosphere at 37 °C with 5% CO_2.

Cytotoxicity Studies. The cytotoxicity of monoisoprenoyl Ptx NPs and Ptx was investigated by MTT [3-(4,5-dimethylthiazol-2-yl)-2,5-diphenyl tetrazolium bromide] viability test on MiaPaCa-2, A549 and MCF7 cell lines. Briefly, 3000 cells per well were incubated in 100 μL of complete culture medium in 96-well plates for 24 h. The cells were then exposed to a series of concentrations of NPs or free Ptx for 72 h. At the end of the incubation period 20 μL of a 5 mg.mL^{-1} MTT (Sigma Aldrich, Germany) solution in phosphate buffered saline was added to each well. Two h incubation later, the culture medium was gently aspirated and replaced by 200 μL of dimethylsulfoxide (ACS grade, BioBasic Inc., France) in order to dissolve the formazan crystals. The absorbance of the solubilized dye was measured spectrophotometrically with a microplate reader (LAB Systems Original Multiscan MS, Finland) at 570 nm. The percentage of viable cells in each well was calculated as the absorbance ratio between treated and untreated control cells. The inhibitory concentration 50% (IC_{50}) of the treatments was determined from the dose−response curve. All experiments were set up in triplicate to determine means and SDs.

***In Vivo* Study.** Four to six week old female balb/c mice were purchased from Harlan Laboratory (France). All animals were housed in appropriate animal care facilities during the experimental period, in isolated ventilated racks with free access to food and water, and were handled according to the principles of laboratory animal care and legislation in force in France. The systemic toxicity of the PtxMIP_SQ-PEG NPs was first investigated on healthy mice, comparatively to paclitaxel by determining the maximum tolerated dose (MTD) after repeated intravenous injection. The MTD was estimated based on the threshold at which all animals survived with a body weight loss less than 10%. Practically, animals received five intravenous injections on days 0, 1, 2, 3, and 4 in the lateral tail vein (10 μL.g^{-1} of body weight). Six groups of balb/c mice received monoisoprenoyl paclitaxel NPs at a paclitaxel equivalent dose of 5, 10, 15, 20, 25, or 30 mg.kg^{-1}; and six groups of balb/c mice received paclitaxel at a dose of 5, 10, 15, 20, 25, or 30 mg.kg^{-1}. Paclitaxel solution was prepared by dissolving 6 mg of Ptx in 1 mL of Cremophor EL/dehydrated ethanol mixture (50/50 v/v), further diluted to 1.5 mg.mL^{-1} with 5% dextrose solution before administration (i.e., corresponding to the formulation and administration conditions of Taxol). The body weight change and physical status of mice were monitored for a period of 29 days.

The antitumor efficacy of PtxMIP_SQ-PEG NPs and paclitaxel was further evaluated at equitoxic doses (i.e., MTD). Practically, 200 μL of the 4T1-luc cell suspension, equivalent to 1.5 × 10^5 cells, was injected intravenously in the lateral vein, to obtain a breast cancer lung metastasis model. Three days after injection of 4T1-luc cells, mice were randomized according to bioluminescence intensity in the lungs and assigned into 3 groups of 12 mice each and all groups received five intravenous injections on days 0, 1, 2, 3, and 4 in the lateral vein with (i) PtxMIP_SQ-PEG NPs at paclitaxel equivalent dose of 25 mg.kg^{-1}, (ii) paclitaxel at dose of 15 mg.kg^{-1}, or (iii) 5% dextrose control solution. The injected volume was 10 μL.g^{-1} of body weight. The mice were monitored regularly for changes in weight and health status. Mice were humanely sacrificed 48 h after the last treatment. *Ex-vivo* pictures of excised lung were taken with a digital photocamera.

Bioluminescence Imaging. BLI was performed before the first treatment and then every two days (day 0, 2, 4 and 6) using the IVIS-Lumina-II imaging system (PerkinElmer, Roissy, France). Mice were injected intraperitoneally with luciferin potassium salt (Promega, France) at a dose of 100 mg.kg^{-1} and imaged after 6 min. Animals under gaseous anesthesia (2% vaporized isofluorane) were placed inside the dark box of a high sensitivity charge coupled device camera cooled to −90 °C. Acquisition settings (binning and duration) were set up depending upon tumor activity. Signal intensity was quantified as the sum of all photons detected from both the ventral and dorsal positions within a manually drawn region of interest.

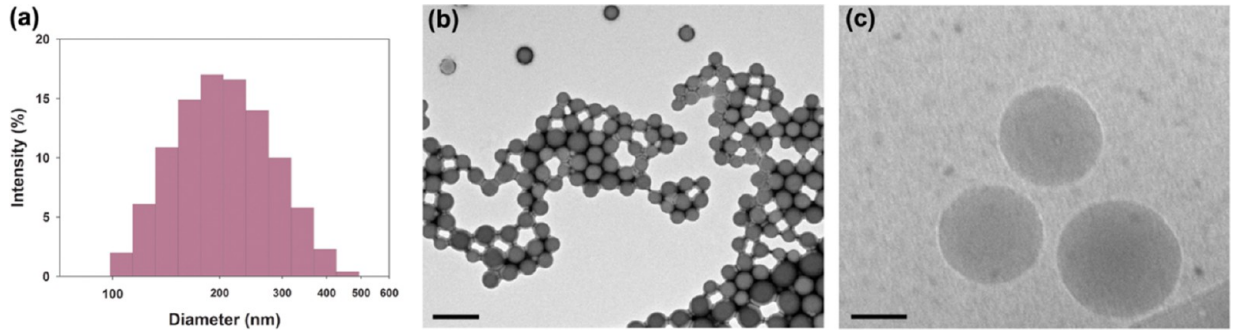

Figure 1. Dynamic light scattering (DLS) data giving the average diameter in intensity (a); transmission electron microscopy (TEM) (b); and cryogenic transmission electron microscopy (Cryo-TEM) (c) of PtxMIP_SQ-PEG NPs. Scale bars: 500 nm (b) and 100 nm (c).

Emitted light was measured using the Living Image software (PerkinElmer, Roissy, France).

RESULTS AND DISCUSSION

Compound **2** was simply prepared by acylation of Paclitaxel (**1**) with 5-methyl-hex-4-enoic acid (**3**) using DCC/DMAP as coupling agent taking into account the difference in reaction rates between the PTX 2′- and 7-OH groups.[31] Under these conditions only a minute amount of 2′,7-diacylated products was observed and the product was easily purified by column chromatography. Interestingly the use of EDCI/DMAP was found less selective giving a significant amount of 2′,7-diacylated material.

Table 1. Anticancer Activity of PtxMIP_SQ-PEG Nanoparticles and Ptx after 72 h Incubation (Expressed as IC_{50} ± SD in nM)[a]

cell line	PtxMIP_SQ-PEG NPs	Ptx
MCF7	238 ± 31	25 ± 3
A549	187 ± 17	16 ± 1
Mia PaCa-2	85 ± 5	8 ± 1

[a]Determined by cell viability assay (MTT test).

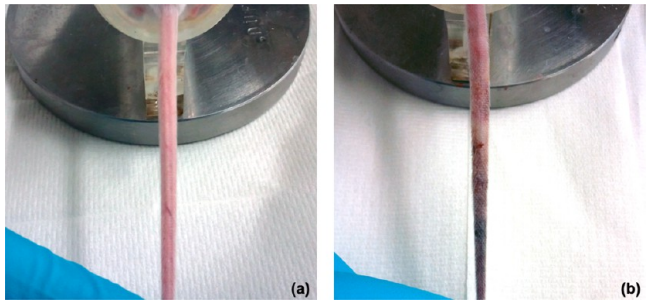

Figure 2. Images of the tail of representative mice after 5 consecutive injections of PtxMIP_SQ-PEG NPs (a) and free Ptx at 25 mg.kg^{-1} (b).

Nanoparticles (NPs) were prepared by co-nanoprecipitation in water of an ethanolic solution of the resulting bioconjugate **2** mixed with SQ-PEG, followed by ethanol evaporation under vacuum. The obtained milky dispersion (4 mg.mL^{-1}) contained NPs with a mean diameter of 190−210 nm and a narrow particle size distribution (0.08 ± 0.03) (Figure 1a). NPs were found to be negatively charged with a mean ζ-potential value of around −15 mV. The isoprenoyl Ptx NPs showed an impressively high drug loading (82%), while conventional

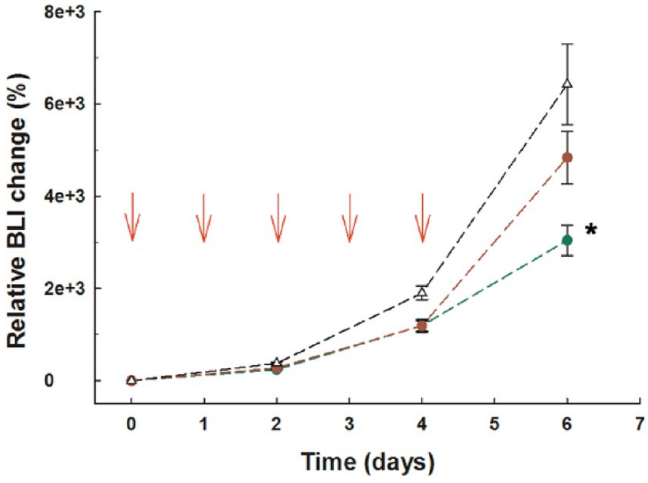

Figure 3. Tumor progression monitored by BLI as a function of time following intravenous administration of PtxMIP_SQ-PEG NPs (green - -●- -, 25 mg.kg^{-1} Ptx equivalent dose), Ptx (red - -●- -, 15 mg.kg^{-1}), and control 5% dextrose solution (--Δ--). Values represent means ± SEM, n = 12, for each group. Red arrows indicate the injection days. Statistical difference between PtxMIP_SQ-PEG NPs and Ptx-treated groups (Student's t-test with Bonferroni correction for multiple comparisons) is marked by * ($p < 0.05$).

colloidal formulations of Ptx rarely achieved drug payloads higher than a few percent. In addition, formulated NPs showed physical stability for an extended period of time at 4 °C (up to six months). On the contrary, when nanoprecipitation was performed using the free drug instead of the bioconjugate, Ptx immediately precipitated in the aqueous phase forming typical needle crystals. These results highlight the crucial contribution of just a single isoprene moiety to the physicochemical behavior of the bioconjugate. PtxMIP_SQ-PEG NPs were highly stable also at room temperature as well as at 37 °C, with no significant variation of their mean diameter both at different pH values (i.e., pH 4.5 and pH 9.1) and in a cell culture medium, over a period of 21 days. A lower stability was, however, observed at pH 7.4, which caused size increase and larger particle size distribution but only after 21 days at room temperature and after 24 h at 37 °C (Figure S1, S2). Size of nanoparticles was confirmed by transmission electron microscopy (TEM) (Figure 1b) and cryo-transmission electron microscopy (Cryo-TEM) (Figure 1c), which revealed spherical-shaped structures, with mean diameters and size-distribution in good agreement with the dynamic light scattering. According to the particle size and the PEG content, it was possible to calculate that the surface area available for each PEG chain at the surface of the NPs was

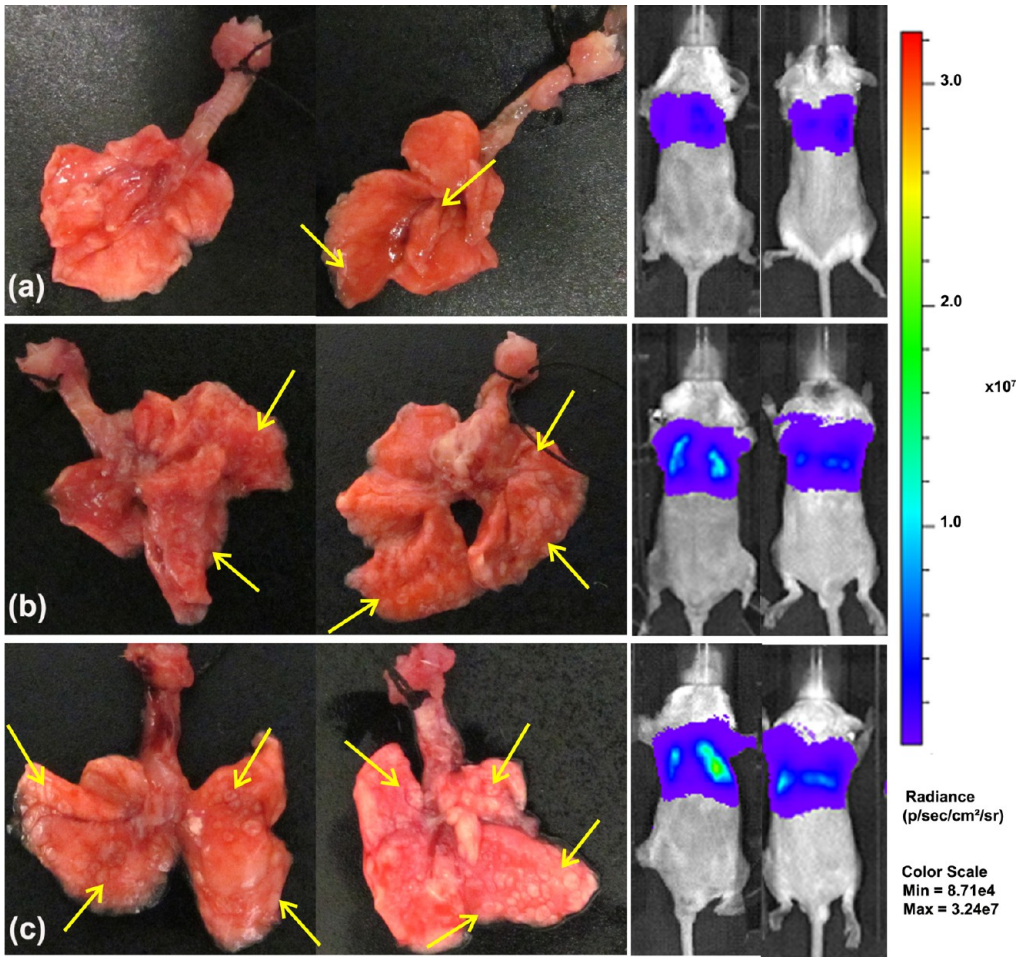

Figure 4. *Ex vivo* exemplificative pictures of excised lung and bioluminescent images of mice treated with the PtxMIP_SQ-PEG NPs (a), free Ptx (b), and control 5% dextrose solution (c). Metastasis can be identified as white spots (see arrows).

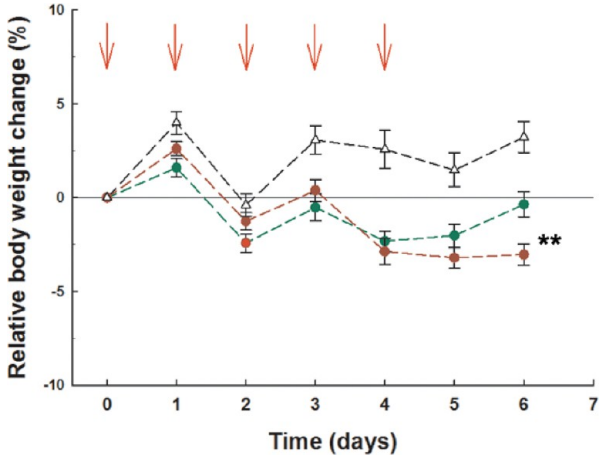

Figure 5. Relative body weight change as a function of time following intravenous administration of PtxMIP_SQ-PEG NPs (green - -●- -, 25 mg.kg^{-1} Ptx equivalent dose), Ptx (red - -●- -, 15 mg.kg^{-1}), and control 5% dextrose solution (--Δ--). Values represent means ± SEM, n = 12, for each group. Red arrows indicate the injection days. Statistical difference between PtxMIP_SQ-PEG NPs and Ptx-treated groups (Student's t-test with Bonferroni correction for multiple comparisons) is marked by ** (p < 0.02).

of 1.23 nm^2, which corresponded to a distance of 1.11 nm between two neighboring PEG chains. In agreement with the literature,[75] a value below 2.2 nm is expected to enhance NPs stability in the blood compartment and prevent the adsorption of plasma proteins on their surface, thus prolonging NPs blood circulation time, due to reduction of macrophage uptake.[76,77] Incubation of PtxMIP_SQ-PEG NPs in human serum resulted in a very low release of free Ptx. After 72 h of incubation at 37 °C, approximately 1.3% of the total paclitaxel content was released (Figure S3). Despite these *in vitro* data and because it is well documented that esterification at C-2′ OH of paclitaxel results in a loss of microtubule protein assembly activity, leading to an inactive conjugate that requires hydrolysis back to paclitaxel to be active,[31−34,36] it is suggested that paclitaxel should, however, be released *in vivo* to allow the cytotoxic activity of PtxMIP_SQ-PEG NPs to be exerted, as previously reported also by other groups,[35,60,61,78] The more aggressive *in vivo* intracellular enzymatic content, comparatively to serum, the possible inhibition *in vitro* of serum enzymes after 72 h incubation as well as the fact that the *in vitro* release experiment was performed over a shorter period compared to the length of the *in vivo* efficacy experiment, may account for a more important release of paclitaxel in *in vivo* conditions.

The cytotoxic activity of monoisoprenoyl Ptx nanoparticles (PtxMIP_SQ-PEG NPs) was assessed *in vitro* on three human cancer cell lines (i.e., hormone-dependent breast adenocarcinoma cells (MCF 7), lung adenocarcinoma cells (A549), and pancreatic adenocarcinoma cells (MIA PACA-2)), using free Ptx as a control. Half maximal inhibitory concentration (IC_{50})

dx.doi.org/10.1021/bc400210x | *Bioconjugate Chem.* 2013, 24, 1840−1849

values are reported in Table 1. As expected, owing to their prodrug nature, PtxMIP_SQ-PEG nanoparticles showed lower cytotoxicity (around 10-fold) compared to the free drug, which was active in the nanomolar range. Noteworthy is that the cytotoxic activity of PtxMIP_SQ-PEG NPs was significantly increased compared to the Ptx-SQ NPs, which showed IC_{50} values of 1750, 2700, and 450 nM in MCF7, A549, and MiaPACA-2 cells, respectively.[70] This highlights that a short isoprene chain may provide the Ptx prodrug with an improved activity on these cancer cells, maintaining the ability to self-assemble as nanoparticles.

According to the approved use of paclitaxel as a first line treatment in woman with advanced breast cancer,[79] the antitumor activity of the PtxMIP_SQ-PEG NPs was then assessed *in vivo* in a murine model of lung metastatic mammary carcinoma in balb/c mice. The 4T1 breast cells, which derived from a spontaneously arising balb/c mammary tumor,[80] were injected intravenously to mice in order to develop a lung mestastatic model of stage IV breast cancer.[81,82] In this study, 4T1 cells which stably integrated the luciferase gene were used in order to allow noninvasive quantitative monitoring of tumor progression by bioluminescence imaging (BLI) during the whole experiment period.

In a preliminary experiment, the systemic toxicity of both Ptx free and PtxMIP_SQ-PEG NPs was determined in healthy mice by measuring the maximum tolerated dose (MTD, i.e., the threshold at which all animals survived with a body weight loss less than 10%). MTD was found to be 25 $mg.kg^{-1}$ (equiv Ptx) for PtxMIP_SQ-PEG NPs and 15 $mg.kg^{-1}$ for free Ptx. Moreover, after 5 intravenous injections of PtxMIP_SQ-PEG NPs at 25 $mg.kg^{-1}$ (equiv Ptx), no visible tissue irritation could be observed at the injection site (Figure 2a), whereas hypersensitivity reaction, with clear necrosis of soft tissues, ulceration, edema, and erythema, was observed in the group treated with free Ptx formulation containing Cremophor (Figure 2b). According to those toxicity investigations, the treatment of the tumor-bearing animals was further performed at the MTD value (i.e., 25 $mg.kg^{-1}$ (equiv Ptx) for PtxMIP_SQ-PEG NPs and 15 $mg.kg^{-1}$ for free Ptx formulation).

According to the rapid 4T1 cells growth, the first bioluminescence investigation was performed three days after cell injection (lung bioluminescence signal was measured in 100% of mice). Immediately afterward, according to the *in vivo* bioluminescence intensity, mice were randomized into treatment and control groups, and received the first treatment (d = 0). Bioluminescence imaging was then performed every two days (day 0, 2, 4, and 6). Mice received a total of 5 intravenous injections at MTD (corresponding to a cumulative dose of 125 $mg.kg^{-1}$ (equiv Ptx) of PtxMIP_SQ-PEG NPs and 75 $mg.kg^{-1}$ of Ptx free drug).

After 5 days treatment, BLI analysis showed a significant reduction of the lung intensity (corresponding to the metastatic dissemination rate) in mice treated with PtxMIP_SQ-PEG NPs, as compared to free drug or control (i.e., 5% dextrose)-receiving groups (Figure 3). Bioluminescent imaging pictures and *ex vivo* photographic images of excised lungs confirmed the slower formation of metastatic nodules in mice treated with the prodrug formulation (Figure 4). Still, complete inhibition of the metastatic spread was not observed. According to body weight change, it was observed that monoisoprenoyl Ptx NPs, even at higher dose (MTD 25 $mg.kg^{-1}$ vs 15 $mg.kg^{-1}$ for the free drug), were better tolerated than the conventional Ptx formulation. Indeed, although a decrease of the body weight was observed in both groups during the treatment period, mice treated with PtxMIP_SqPEG NPs had already recovered initial weight 48 h after the last injection, which was not the case with free Ptx (Figure 5).

CONCLUSIONS

The chemical linkage of a single isoprene unit to paclitaxel was found to enable, in the presence of SQ-PEG, the self-assembly of the resulting paclitaxel−isoprene conjugate as nanoparticles decorated with polyethylene glycol and carrying an impressively high drug payload. This formulation was better tolerated than the conventional Ptx Cremophor-containing formulation, thus allowing administration of higher doses. In addition, the prodrug nanoformulation slowed the metastatic burden in the lungs and showed a higher safety compared to the free drug. In a nutshell, the single addition of a monoisoprenoyl unit to paclitaxel allowed design of a novel promising nanoassembled prodrug which opens the way for further pharmacological studies.

ASSOCIATED CONTENT

Supporting Information

Colloidal and chemical stability of PtxMIP_SQ-PEG NPs. This material is available free of charge via the Internet at http://pubs.acs.org.

AUTHOR INFORMATION

Corresponding Authors

*E-mail: simona.mura@u-psud.fr; Tel: +33 1 46 83 58 19; Fax: +33 1 46 83 55 11.

*E-mail: patrick.couvreur@u-psud.fr; Tel: +33 1 46 83 53 96; Fax: +33 1 46 83 55 11.

Present Address

Davide Brambilla, Institute of Pharmaceutical Sciences, Swiss Federal Institute of Technology, ETH Zurich, Wolfgang-Pauli-Str. 10, HCI H303, CH-8093 Zurich, Switzerland

Notes

The authors declare no competing financial interest.

ACKNOWLEDGMENTS

The authors warmly thank Dr. Claire Boulogne for the TEM analysis ((Electron Microscopy Platform) Cell biology unit of the Imagif platform (Centre de Recherche de Gif)) and Ghislaine Frébourg (Service of Electron Microscopy from IFR of Integrative Biology, Paris) for the cryo-TEM analysis. Simona Mura wishes to thank Marilyne Le Mée, Stéphanie Retif, Julien Sobilo, Dr. Laura Brullé, Dr. Sabrina Pesnel, and Dr. Marc Vandamme (TAAM-UPS44, CIPA, CNRS Orléans) for full-time training and fruitful discussions.The research leading to these results has received funding from the European Research Council under the European Community's Seventh Framework Programme FP7/2007-2013 Grant Agreement No. 249835. The CNRS and the French Ministry of Research are also warmly acknowledged for financial support.

ABBREVIATIONS USED

Ptx, Paclitaxel; DHA-Ptx, docosahexaenoic-acid-Paclitaxel; SQ, squalene; SQ-PEG, Trisnorsqualene-Me polyethylene glycol; PtxMIP, monoisoprenoyl paclitaxel; DCC, dicyclohexylcarbodiimide; DMAP, 4-dimethylaminopyridine; EDCI, 1-ethyl-3-(3-dimethylaminopropyl)carbodiimide; MTT, 3-(4,5-dimethylth-

iazol-2-yl)-2,5-diphenyltetrazoliumbromide; DLS, dynamic light scattering; TEM, transmission electron microscopy; Cryo-TEM, cryogenic transmission electron microscopy; NP, nanoparticle; BLI, bioluminescence imaging; MTD, maximum tolerated dose; IR, infrared; ESI, electron spray ionization; SD, standard deviation; SEM, standard error of the mean; IC_{50}, half maximal inhibitory concentration

REFERENCES

(1) Wani, M. C., Taylor, H. L., Wall, M. E., Coggon, P., and McPhail, A. T. (1971) Plant antitumor agents. VI. Isolation and structure of taxol, a novel antileukemic and antitumor agent from Taxus brevifolia. *J. Am. Chem. Soc. 93*, 2325−2327.

(2) Spencer, C. M., and Faulds, D. (1994) Paclitaxel. A review of its pharmacodynamic and pharmacokinetic properties and therapeutic potential in the treatment of cancer. *Drugs 48*, 794−847.

(3) Schiff, P. B., Fant, J., and Horwitz, S. B. (1979) Promotion of microtubule assembly in vitro by taxol. *Nature 277*, 665−667.

(4) Liggins, R. T., Hunter, W. L., and Burt, H. M. (1997) Solid-state characterization of paclitaxel. *J. Pharm. Sci. 86*, 1458−1463.

(5) Gelderblom, H., Verweij, J., Nooter, K., and Sparreboom, A. (2001) Cremophor EL: the drawbacks and advantages of vehicle selection for drug formulation. *Eur. J. Cancer 37*, 1590−1598.

(6) Lorenz, W., Reimann, H. J., Schmal, A., Dormann, P., Schwarz, B., Neugebauer, E., and Doenicke, A. (1977) Histamine release in dogs by Cremophor E1 and its derivatives: oxethylated oleic acid is the most effective constituent. *Agents Actions 7*, 63−67.

(7) Szebeni, J., Muggia, F. M., and Alving, C. R. (1998) Complement activation by Cremophor EL as a possible contributor to hypersensitivity to paclitaxel: an in vitro study. *J. Natl. Cancer Inst. 90*, 300−306.

(8) ten Tije, A. J., Verweij, J., Loos, W. J., and Sparreboom, A. (2003) Pharmacological effects of formulation vehicles - Implications for cancer chemotherapy. *Clin. Pharmacokinet. 42*, 665−685.

(9) Wiernik, P. H., Schwartz, E. L., Strauman, J. J., Dutcher, J. P., Lipton, R. B., and Paietta, E. (1987) Phase I clinical and pharmacokinetic study of taxol. *Cancer Res. 47*, 2486−2493.

(10) Weiss, R. B., Donehower, R. C., Wiernik, P. H., Ohnuma, T., Gralla, R. J., Trump, D. L., Baker, J. R., Jr., Van Echo, D. A., Von Hoff, D. D., and Leyland-Jones, B. (1990) Hypersensitivity reactions from taxol. *J. Clin. Oncol. 8*, 1263−1268.

(11) Knemeyer, I., Wientjes, M. G., and Au, J. L. S. (1999) Cremophor reduces paclitaxel penetration into bladder wall during intravesical treatment. *Cancer Chemother. Pharmacol. 44*, 241−248.

(12) Ng, S. S. W., Figg, W. D., and Sparreboom, A. (2004) Taxane-mediated antiangiogenesis in vitro: Influence of formulation vehicles and binding proteins. *Cancer Res. 64*, 821−824.

(13) Sparreboom, A., van Zuylen, L., Brouwer, E., Loos, W. J., de Bruijn, P., Gelderblom, H., Pillay, M., Nooter, K., Stoter, G., and Verweij, J. (1999) Cremophor EL-mediated alteration of paclitaxel distribution in human blood: clinical pharmacokinetic implications. *Cancer Res. 59*, 1454−1457.

(14) Lundberg, B. B. (1997) A submicron lipid emulsion coated with amphipathic polyethylene glycol for parenteral administration of paclitaxel (Taxol). *J. Pharm. Pharmacol. 49*, 16−21.

(15) Sharma, A., and Straubinger, R. M. (1994) Novel taxol formulations - preparation and characterization of taxol-containing liposomes. *Pharm. Res. 11*, 889−896.

(16) Koudelka, Š., and Turánek, J. (2012) Liposomal paclitaxel formulations. *J. Controlled Release 163*, 322−334.

(17) Alkanonyuksel, H., Ramakrishnan, S., Chai, H. B., and Pezzuto, J. M. (1994) A mixed micellar formulation suitable for the parenteral administration of taxol. *Pharm. Res. 11*, 206−212.

(18) Lee, S. C., Huh, K. M., Lee, J., Cho, Y. W., Galinsky, R. E., and Park, K. (2007) Hydrotropic polymeric micelles for enhanced paclitaxel solubility: in vitro and in vivo characterization. *Biomacromolecules 8*, 202−208.

(19) Shuai, X. T., Merdan, T., Schaper, A. K., Xi, F., and Kissel, T. (2004) Core-cross-linked polymeric micelles as paclitaxel carriers. *Bioconjugate Chem. 15*, 441−448.

(20) Wang, T., Petrenko, V. A., and Torchilin, V. P. (2010) Paclitaxel-loaded polymeric micelles modified with MCF-7 cell-specific phage protein: enhanced binding to target cancer cells and increased cytotoxicity. *Mol. Pharmaceutics 7*, 1007−1014.

(21) Jiang, X., Xin, H., Sha, X., Gu, J., Jiang, Y., Law, K., Chen, Y., Chen, L., Wang, X., and Fang, X. (2011) PEGylated poly(trimethylene carbonate) nanoparticles loaded with paclitaxel for the treatment of advanced glioma: in vitro and in vivo evaluation. *Int. J. Pharm. 420*, 385−394.

(22) Koziara, J. M., Lockman, P. R., Allen, D. D., and Mumper, R. J. (2004) Paclitaxel nanoparticles for the potential treatment of brain tumors. *J. Controlled Release 99*, 259−269.

(23) Yeh, T. K., Lu, Z., Wientjes, M. G., and Au, J. L. S. (2005) Formulating paclitaxel in nanoparticles alters its disposition. *Pharm. Res. 22*, 867−874.

(24) Letchford, K., and Burt, H. M. (2012) Copolymer micelles and nanospheres with different in vitro stability demonstrate similar paclitaxel pharmacokinetics. *Mol. Pharm. 9*, 248−260.

(25) Bhardwaj, V., Ankola, D. D., Gupta, S. C., Schneider, M., Lehr, C. M., and Kumar, M. N. (2009) PLGA nanoparticles stabilized with cationic surfactant: safety studies and application in oral delivery of paclitaxel to treat chemical-induced breast cancer in rat. *Pharm. Res. 26*, 2495−2503.

(26) Lo, S. T., Stern, S., Clogston, J. D., Zheng, J., Adiseshaiah, P. P., Dobrovolskaia, M., Lim, J., Patri, A. K., Sun, X., and Simanek, E. E. (2010) Biological assessment of triazine dendrimer: toxicological profiles, solution behavior, biodistribution, drug release and efficacy in a PEGylated, paclitaxel construct. *Mol. Pharmaceutics 7*, 993−1006.

(27) Ooya, T., Lee, J., and Park, K. (2003) Effects of ethylene glycol-based graft, star-shaped, and dendritic polymers on solubilization and controlled release of paclitaxel. *J. Controlled Release 93*, 121−127.

(28) Gradishar, W. J., Tjulandin, S., Davidson, N., Shaw, H., Desai, N., Bhar, P., Hawkins, M., and O'Shaughnessy, J. (2005) Phase III trial of nanoparticle albumin-bound paclitaxel compared with polyethylated castor oil-based paclitaxel in women with breast cancer. *J. Clin. Oncol. 23*, 7794−7803.

(29) Fu, Q., Sun, J., Zhang, W. P., Sui, X. F., Yan, Z. T., and He, Z. G. (2009) Nanoparticle albumin-bound (NAB) technology is a promising method for anti-cancer drug delivery. *Recent Pat. Anti-Cancer 4*, 262−272.

(30) Lee, K. S., Chung, H. C., Im, S. A., Park, Y. H., Kim, C. S., Kim, S. B., Rha, S. Y., Lee, M. Y., and Ro, J. (2008) Multicenter phase II trial of Genexol-PM, a Cremophor-free, polymeric micelle formulation of paclitaxel, in patients with metastatic breast cancer. *Breast Cancer Res. Treat. 108*, 241−250.

(31) Deutsch, H. M., Glinski, J. A., Hernandez, M., Haugwitz, R. D., Narayanan, V. L., Suffness, M., and Zalkow, L. H. (1989) Synthesis of congeners and prodrugs. 3. Water-soluble prodrugs of taxol with potent antitumor activity. *J. Med. Chem. 32*, 788−792.

(32) Kingston, D. G. (2000) Recent advances in the chemistry of taxol. *J. Nat. Prod. 63*, 726−734.

(33) Zhu, Q., Guo, Z., Huang, N., Wang, M., and Chu, F. (1997) Comparative molecular field analysis of a series of paclitaxel analogues. *J. Med. Chem. 40*, 4319−4328.

(34) Lataste, H., Senilh, V., Wright, M., Guénard, D., and Potier, P. (1984) Relationships between the structures of taxol and baccatine III derivatives and their in vitro action on the disassembly of mammalian brain and Physarum amoebal microtubules. *Proc. Natl. Acad. Sci. U.S.A. 81*, 4090−4094.

(35) Ueda, Y., Wong, H., Matiskella, J. D., Mikkilineni, A. B., Farina, V., Fairchild, C., Rose, W. C., Mamber, S. W., Long, B. H., Kerns, E. H., Casazza, A. M., and Vyas, D. M. (1994) Synthesis and antitumor evaluation of 2′-oxycarbonylpaclitaxels (paclitaxel-2′-carbonates). *Bioorg. Med. Chem. Lett. 4*, 1861−1864.

(36) Kingston, D. G. I. (1994) Taxol: The chemistry and structure-activity relationships of a novel anticancer agent. *Trends Biotechnol. 12*, 222−227.
(37) Paradis, R., and Page, M. (1998) New active paclitaxel amino acids derivatives with improved water solubility. *Anticancer Res. 18*, 2711−2716.
(38) Nicolaou, K. C., Riemer, C., Kerr, M. A., Rideout, D., and Wrasidlo, W. (1993) Design, synthesis and biological activity of protaxols. *Nature 364*, 464−466.
(39) Zhao, Z., Kingston, D. G. I., and Crosswell, A. R. (1991) Modified taxols, 6. preparation of water-soluble prodrugs of taxol. *J. Nat. Prod. 54*, 1607−1611.
(40) Rose, W. C., Clark, J. L., Lee, F. Y., and Casazza, A. M. (1997) Preclinical antitumor activity of water-soluble paclitaxel derivatives. *Cancer Chemother. Pharmacol. 39*, 486−492.
(41) Ueda, Y., Mikkilineni, A. B., Knipe, J. O., Rose, W. C., Casazza, A. M., and Vyas, D. M. (1993) Novel water-soluble phosphate prodrugs of Taxol(R) possessing in-vivo antitumor-activity. *Bioorg. Med. Chem. Lett. 3*, 1761−1766.
(42) deBont, D. B. A., Leenders, R. G. G., Haisma, H. J., vanderMeulenMuileman, I., and Scheeren, H. W. (1997) Synthesis and biological activity of beta-glucuronyl carbamate-based prodrugs of paclitaxel as potential candidates for ADEPT. *Bioorg. Med. Chem. 5*, 405−414.
(43) Takahashi, T., Tsukamoto, H., and Yamada, H. (1998) Design and synthesis of a water-soluble taxol analogue: taxol-sialyl conjugate. *Bioorg. Med. Chem. Lett. 8*, 113−116.
(44) Lee, H., Lee, K., and Park, T. G. (2008) Hyaluronic acid-paclitaxel conjugate micelles: Synthesis, characterization, and anti-tumor activity. *Bioconjugate Chem. 19*, 1319−1325.
(45) Wang, Y., Xin, D., Liu, K., Zhu, M., and Xiang, J. (2009) Heparin−paclitaxel conjugates as drug delivery system: synthesis, self-assembly property, drug release, and antitumor activity. *Bioconjugate Chem. 20*, 2214−2221.
(46) Wang, S. D., Zhelev, N. Z., Duff, S., and Fischer, P. M. (2006) Synthesis and biological activity of conjugates between paclitaxel and the cell delivery vector penetratin. *Bioorg. Med. Chem. Lett. 16*, 2628−2631.
(47) Li, C., Yu, D. F., Newman, R. A., Cabral, F., Stephens, L. C., Hunter, N., Milas, L., and Wallace, S. (1998) Complete regression of well-established tumors using a novel water-soluble poly(L-glutamic acid)-paclitaxel conjugate. *Cancer Res. 58*, 2404−2409.
(48) Papas, S., Akoumianaki, T., Kalogiros, C., Hadjiarapoglou, L., Theodoropoulos, P. A., and Tsikaris, V. (2007) Synthesis and antitumor activity of peptide-paclitaxel conjugates. *J. Pept. Sci. 13*, 662−671.
(49) Kirschberg, T. A., VanDeusen, C. L., Rothbard, J. B., Yang, M., and Wender, P. A. (2003) Arginine-based molecular transporters: the synthesis and chemical evaluation of releasable taxol-transporter conjugates. *Org. Lett. 5*, 3459−3462.
(50) Chen, X. Y., Plasencia, C., Hou, Y. P., and Neamati, N. (2005) Synthesis and biological evaluation of dimeric RGD peptide-paclitaxel conjugate as a model for integrin-targeted drug delivery. *J. Med. Chem. 48*, 1098−1106.
(51) Safavy, A., Raisch, K. P., Khazaeli, M. B., Buchsbaum, D. J., and Bonner, J. A. (1999) Taxane derivatives for targeted therapy of cancer: Design and synthesis of a soluble paclitaxel-peptide conjugate with enhanced antitumor activity. *Clin. Cancer Res. 5*, 3820s−3820s.
(52) Sohn, J. S., Jin, J. I., Hess, M., and Jo, B. W. (2010) Polymer prodrug approaches applied to paclitaxel. *Polym. Chem. 1*, 778−792.
(53) Greenwald, R. B., Gilbert, C. W., Pendri, A., Conover, C. D., Xia, J., and Martinez, A. (1996) Drug delivery systems: water soluble taxol 2′-poly(ethylene glycol) ester prodrugs-design and in vivo effectiveness. *J. Med. Chem. 39*, 424−431.
(54) Etrych, T., Sirova, M., Starovoytova, L., Rihova, B., and Ulbrich, K. (2010) HPMA copolymer conjugates of paclitaxel and docetaxel with pH-controlled drug release. *Mol. Pharmaceutics 7*, 1015−1026.
(55) Hostetler, K. Y. Sridhar, N. C. Prodrugs for Oral Administration Containing Taxol Covalently Bound to a Phospholipid. U.S. Patent 5,484,809, January 16, 1996.
(56) Ansell, S. Lipophilic Drug Derivatives for Use in Liposomes. U.S. Patent 5,534,499, July 9, 1996.
(57) Perkins, W. R., Ahmad, I., Li, X. G., Hirsh, D. J., Masters, G. R., Fecko, C. J., Lee, J. K., Ali, S., Nguyen, J., Schupsky, J., Herbert, C., Janoff, A. S., and Mayhew, E. (2000) Novel therapeutic nano-particles (lipocores): trapping poorly water soluble compounds. *Int. J. Pharm. 200*, 27−39.
(58) Stevens, P. J., Sekido, M., and Lee, R. J. (2004) A folate receptor-targeted lipid nanoparticle formulation for a lipophilic paclitaxel prodrug. *Pharm. Res. 21*, 2153−2157.
(59) Ali, S., Ahmad, I., Peters, A., Masters, G., Minchey, S., Janoff, A., and Mayhew, E. (2001) Hydrolyzable hydrophobic taxanes: synthesis and anti-cancer activities. *Anti-Cancer Drugs 12*, 117−128.
(60) Bradley, M. O., Webb, N. L., Anthony, F. H., Devanesan, P., Witman, P. A., Hemamalini, S., Chander, M. C., Baker, S. D., He, L. F., Horwitz, S. B., and Swindell, C. S. (2001) Tumor targeting by covalent conjugation of a natural fatty acid to paclitaxel. *Clin. Cancer Res. 7*, 3229−3238.
(61) Ke, X. Y., Zhao, B. J., Zhao, X., Wang, Y., Huang, Y., Chen, X. M., Zhao, B. X., Zhao, S. S., Zhang, X., and Zhang, Q. (2010) The therapeutic efficacy of conjugated linoleic acid - paclitaxel on glioma in the rat. *Biomaterials 31*, 5855−5864.
(62) Lee, J. W., Lu, J. Y., Low, P. S., and Fuchs, P. L. (2002) Synthesis and evaluation of taxol-folic acid conjugates as targeted antineoplastics. *Bioorg. Med. Chem. 10*, 2397−2414.
(63) Bedikian, A. Y., DeConti, R. C., Conry, R., Agarwala, S., Papadopoulos, N., Kim, K. B., and Ernstoff, M. (2011) Phase 3 study of docosahexaenoic acid−paclitaxel versus dacarbazine in patients with metastatic malignant melanoma. *Ann. Oncol. 22*, 787−793.
(64) Jones, R., Hawkins, R., Eatock, M., Ferry, D., Eskens, F. L. M., Wilke, H., and Evans, T. R. J. (2008) A phase II open-label study of DHA-paclitaxel (Taxoprexin) by 2-h intravenous infusion in previously untreated patients with locally advanced or metastatic gastric or oesophageal adenocarcinoma. *Cancer Chemother. Pharmacol. 61*, 435−441.
(65) Reddy, L. H., and Couvreur, P. (2010) Lipid-Based Anticancer Prodrugs, in *Macromolecular Anticancer Therapeutics*, Springer.
(66) Couvreur, P., Stella, B., Reddy, L. H., Hillaireau, H., Dubernet, C., Desmaele, D., Lepetre-Mouelhi, S., Rocco, F., Dereuddre-Bosquet, N., Clayette, P., Rosilio, V., Marsaud, V., Renoir, J. M., and Cattel, L. (2006) Squalenoyl nanomedicines as potential therapeutics. *Nano Lett. 6*, 2544−2548.
(67) Desmaele, D., Gref, R., and Couvreur, P. (2012) Squalenoylation: a generic platform for nanoparticular drug delivery. *J. Controlled Release 161*, 609−618.
(68) Raouane, M., Desmaele, D., Gilbert-Sirieix, M., Gueutin, C., Zouhiri, F., Bourgaux, C., Lepeltier, E., Gref, R., Ben Salah, R., Clayman, G., Massaad-Massade, L., and Couvreur, P. (2011) Synthesis, characterization, and in vivo delivery of siRNA-squalene nanoparticles targeting fusion oncogene in papillary thyroid carcinoma. *J. Med. Chem. 54*, 4067−4076.
(69) Dosio, F., Reddy, L. H., Ferrero, A., Stella, B., Cattel, L., and Couvreur, P. (2010) Novel nanoassemblies composed of squalenoyl−paclitaxel derivatives: synthesis, characterization, and biological evaluation. *Bioconjugate Chem. 21*, 1349−1361.
(70) Caron, J., Maksimenko, A., Wack, S., Lepeltier, E., Bourgaux, C., Morvan, E., Leblanc, K., Couvreur, P., and Desmaele, D. (2013) Improving the antitumor activity of squalenoyl-paclitaxel conjugate nanoassemblies by manipulating the linker between paclitaxel and squalene. *Adv. Healthcare Mater. 2*, 172−185.
(71) Maksimenko, A., Mougin, J., Mura, S., Sliwinski, E., Lepeltier, E., Bourgaux, C., Lepetre, S., Zouhiri, F., Desmaele, D., and Couvreur, P. (2013) Polyisoprenoyl gemcitabine conjugates self assemble as nanoparticles, useful for cancer therapy. *Cancer Lett. 334*, 346−353.
(72) Harrisson, S., Nicolas, J., Maksimenko, A., Bui, D. T., Mougin, J., and Couvreur, P. (2013) Nanoparticles with in vivo anticancer activity

from polymer prodrug amphiphiles prepared by living radical polymerization. *Angew. Chem., Int. Ed. 52*, 1678−1682.
(73) Menon, S., Sinha-Mahapatra, D., and Herndon, J. W. (2007) Synthesis of phenanthrene derivatives through the net [5 + 5]-cycloaddition of prenylated carbene complexes with 2-alkynylbenzaldehyde derivatives. *Tetrahedron 63*, 8788−8793.
(74) Bekkara-Aounallah, F., Gref, R., Othman, M., Reddy, L. H., Pili, B., Allain, V., Bourgaux, C., Hillaireau, H., Lepêtre-Mouelhi, S., Desmaële, D., Nicolas, J., Chafi, N., and Couvreur, P. (2008) Novel PEGylated nanoassemblies made of self-assembled squalenoyl nucleoside analogues. *Adv. Funct. Mater. 18*, 3715−3725.
(75) Vittaz, M., Bazile, D., Spenlehauer, G., Verrecchia, T., Veillard, M., Puisieux, F., and Labarre, D. (1996) Effect of PEO surface density on long-circulating PLA-PEO nanoparticles which are very low complement activators. *Biomaterials 17*, 1575−1581.
(76) Storm, G., Belliot, S. O., Daemen, T., and Lasic, D. D. (1995) Surface modification of nanoparticles to oppose uptake by the mononuclear phagocyte system. *Adv. Drug Delivery Rev. 17*, 31−48.
(77) Peracchia, M. T., Fattal, E., Desmaele, D., Besnard, M., Noel, J. P., Gomis, J. M., Appel, M., d'Angelo, J., and Couvreur, P. (1999) Stealth PEGylated polycyanoacrylate nanoparticles for intravenous administration and splenic targeting. *J. Controlled Release 60*, 121−128.
(78) Dosio, F., Brusa, P., Crosasso, P., Arpicco, S., and Cattel, L. (1997) Preparation, characterization and properties in vitro and in vivo of a paclitaxel−albumin conjugate. *J. Controlled Release 47*, 293−304.
(79) Yamamoto, Y., Kawano, I., and Iwase, H. (2011) Nab-paclitaxel for the treatment of breast cancer: efficacy, safety, and approval. *Onco Targets Ther. 4*, 123−136.
(80) Aslakson, C. J., and Miller, F. R. (1992) Selective events in the metastatic process defined by analysis of the sequential dissemination of subpopulations of a mouse mammary tumor. *Cancer Res. 52*, 1399−1405.
(81) Tao, K., Fang, M., Alroy, J., and Sahagian, G. G. (2008) Imagable 4T1 model for the study of late stage breast cancer. *BMC Cancer 8*, 228−246.
(82) Miller, F. R. (1983) Tumor subpopulation interactions in metastasis. *Invasion Metastasis 3*, 234−242.

■ NOTE ADDED AFTER ASAP PUBLICATION

This paper was published on the Web on October 17, 2013, with two errors in the first paragraph of the *In Vivo* Study section. The corrected version was reposted on October 22, 2013.